Lifetimes and collision cross sections in the $2p^5 5s$ and $2p^5 4d$ states of neon

J. R. Brandenberger
Department of Physics, Lawrence University, Appleton, Wisconsin 54912
(Received 15 August 1983)

Six lifetimes and eight collisional quenching cross sections $\sigma^{(0)}$ for the $3s_5$, $3s_4$, $3s_3$, $3s_2$, $4d_6$, $4d_5$, $4d_4$, and $4s_1'''$ states in the $2p^5 5s$ and $2p^5 4d$ configurations of neon have been measured using laser-induced time-resolved fluorescence spectroscopy and a weak radio-frequency discharge. Two-step excitation sequences are driven by synchronously pulsed but separately tuned dye lasers. Considerable care is exercised to avoid spurious effects arising from polarized radiation, cascades, and light trapping. The resulting lifetimes vary from 39(4) to 81(6) ns, while the measured cross sections range from 25(4) to 56(4) Å^2. The results are in good agreement with past measurements and theory.

I. INTRODUCTION

Laser-induced time-resolved fluorescence spectroscopy provides a powerful and direct method for measuring excited-state lifetimes in atoms and molecules.[1,2] The reliability of the technique stems mainly from its high state selectivity, which reduces the risk of cascade effects.[3] A recent application of the method to neon[4] involves a pair of synchronously pulsed but separately tuned dye lasers that drive two-step excitations resonantly. Through such two-step excitations, we have been able to reach many high-lying states in neon that have been inaccessible or at least difficult to access in the past in a controlled way. When investigating such states, one usually prefers the clean environment of an atomic beam. The exclusive use of beams is not appropriate in the case of neon, however, because neon has particularly favorable discharge properties that often make it the atom of choice for various plasma experiments. It follows that measurements of the collisional foreshortening of neon lifetimes are nearly as important as the lifetimes themselves, and of course the former must be investigated in a gaseous or plasma target. For these reasons, we have used time-resolved fluorescence spectroscopy and a weak neon discharge to measure the lifetimes and collision cross sections of eight states (the $3s_5$, $3s_4$, $3s_3$, $3s_2$, $4d_6$, $4d_5$, $4d_4$, and $4s_1'''$) in the $2p^5 5s$ and $2p^5 4d$ configurations of neon. Seven of the eight cross sections and two of the lifetimes that we report here are entirely new, they have not been measured before. The remaining lifetimes and cross sections match or exceed in precision the best existing measurements in the literature.

In our experiments, neon atoms confined to a cell in a magnetic field are excited to the $2p^5 3s$ pseudo-ground-states by a weak radio-frequency discharge. A pair of pulsed dye lasers then promote these atoms stepwise into selected levels of the $2p^5 5s$ and $2p^5 4d$ configurations by way of intermediate resonances in the $2p^5 3p$ manifold. Though the ensuing fluorescence is brief, part of it is sufficiently strong and sufficiently well removed from the pumping wavelengths to permit direct photographic capture of the fluorescent signal from an oscilloscope screen. By careful arrangement of the experimental conditions, we ensure that the observed fluorescence consists of a single-exponential decay. The dependence of this decay rate on the background neon pressure is the principal focus of this work.

II. THEORY

Consider the decay of fluorescence from an atomic sample that is excited resonantly by a brief pulse of light at time $t=0$. The assumption that this decay is representable by a single exponential whose decay time is the lifetime of the excited state can be wrong for various reasons: polarization effects associated with the exciting and/or fluorescent radiation, collisional effects that foreshorten lifetimes and redistribute populations, collective effects such as light trapping and coherence narrowing, and cascade effects. These effects must be suppressed or brought under control in any good lifetime measurement. Taking these complications in reverse order, cascade effects can be minimized through the use of selective laser excitation at modest power levels followed by narrow-band observation of part of the fluorescence at a judiciously chosen wavelength. Light trapping, which increases the apparent lifetime of a fluorescent sample, can be suppressed by operating in optically thin samples, or more generally, by ensuring that there is negligible occupancy of all lower states $|c\rangle$ to which a higher state of interest $|b\rangle$ can relax directly. The effects of polarization on the shape of time-resolved fluorescent line shapes have been discussed thoroughly in the literature. When the exciting radiation is plane polarized as in the present work, an atomic sample can exhibit a population decay rate $\Gamma^{(0)}$ as well as an alignment decay rate $\Gamma^{(2)}$, both of which are pressure dependent. In addition, the time-resolved fluorescence may exhibit quantum beats that can jeopardize the reliability of lifetime measurements. Fortunately there is a way to suppress these polarization effects: by observing without any sort of analyzer the fluorescent light emitted parallel to a magnetic field that is normal to the propagation direction of the exciting light, and by orienting the plane of polarization of the exciting light at the "magic angle" $\theta=54.7°$ with respect to the direction of observa-

TABLE I. Two-step excitation sequences and observation channels for the eight states of interest in this work. The A_{ij} are spontaneous transition probabilities in units of 10^8 s^{-1} drawn from Ref. 6; all wavelengths are in Å in air.

Initial state (1)	Excitation (first step) λ_1	A_{12}	Middle state (2)	Excitation (second step) λ_2	A_{23}	State of interest (3)	Observation channel λ_3	A_{34}	Final state (4)
$1s_4$	6383.0	0.321	$2p_7$	6365.0		$3s_5$	5689.8		$2p_{10}$
$1s_4$	6383.0	0.321	$2p_7$	6330.9	0.023	$3s_4$	5662.5	0.007	$2p_{10}$
$1s_3$	6266.5	0.249	$2p_5$	6313.7		$3s_3$	5448.5		$2p_{10}$
$1s_4$	6096.2	0.181	$2p_4$	6328.2	0.034	$3s_2$	5433.7	0.003	$2p_{10}$
$1s_3$	6266.5	0.249	$2p_5$	6172.8		$4d_6$	5343.3		$2p_{10}$
$1s_5$	6143.1	0.282	$2p_6$	6000.9		$4d_5$	5341.1	0.11	$2p_{10}$
$1s_5$	6143.1	0.282	$2p_6$	5991.6		$4d_4$	5820.1		$2p_8$
$1s_5$	5944.8	0.113	$2p_4$	5902.5		$4s_1'''$	5719.2		$2p_6$

tion.[1,2] Although this prescription reduces the amount of observed fluorescence, it must be employed (along with the other conditions stated above) to make sure that the intensity of the fluorescence from state $|b\rangle$ will exhibit a pure exponential decay

$$I(t)=A\exp(-\Gamma^{(0)}t)\ , \tag{1}$$

characterized by the population or "quenching" decay rate $\Gamma^{(0)}$. Assuming the continued absence of cascade effects, this decay rate can be written

$$\Gamma^{(0)}=\gamma_b+n\sigma^{(0)}\bar{v}-\sum_c \gamma_{bc}x_{bc}\alpha_{bc}\ , \tag{2}$$

where the three terms account for unperturbed spontaneous decay, collisional quenching, and light trapping, respectively. The constant $\gamma_b=1/\tau$ is the reciprocal of the lifetime τ of the state $|b\rangle$, n is the density of collisional perturbers (virtually all of which are ground-state neon atoms in this work), $\sigma^{(0)}$ is the average cross section of state $|b\rangle$ for collisional quenching, and $\bar{v}$ is the average relative velocity of the atoms in the sample. In the final term of Eq. (2), the α_{bc} and γ_{bc} are angular factors and specific decay rates to lower states $|c\rangle$ while the x_{bc} are probabilities of reabsorption of fluorescent photons. In the present work, the x_{bc} are either large (in the case of the $3s_2$ and $3s_4$ states because these levels are connected directly to the ground state) or negligible due to low excited-state populations. In the latter case, Eq. (2) can be rewritten as

$$\Gamma^{(0)}=\gamma_b+\beta P\ , \tag{3}$$

where $\beta=\sigma^{(0)}\bar{v}/kT$ is the decay gradient and P is the pressure of the neon sample. Careful measurements in previous investigations[5] have shown that the temperature in our neon samples is $T=340(20)$ K. It follows that $\sigma^{(0)}=4.19\beta$, where the units of $\sigma^{(0)}$ are Å^2 and β are Mrad s^{-1} Torr^{-1}.

Equations (1) and (3) serve as the working equations for this investigation: The first is least-squares fitted to numerous time-resolved experimental line shapes to infer the value of the decay constant $\Gamma^{(0)}$ at various known neon pressures P. These values of $\Gamma^{(0)}$ are then analyzed using Eq. (3) to infer the cross sections $\sigma^{(0)}$ via the decay gradients β. Finally, the unperturbed lifetimes τ are determined from the zero-pressure intercepts γ_b.

III. EXPERIMENT

The excitation sequences and observation channels for the eight states of interest are shown in Table I. All laser excitations commence in the $1s_3$, $1s_4$ or $1s_5$ pseudo-ground states and proceed through one of the $2p$ levels to the "state of interest" identified in the seventh column. All known transition probabilities[6] have been included to indicate the strengths of some of the transitions. The most important single requirement for the observation of these signals is that the final spontaneous transition probability be reasonably strong at a wavelength several hundred angstroms removed from the pumping wavelengths λ_1 and λ_2, and several hundred angstroms removed from all emissions originating in the intermediate state. If this condition is not met, the observed signal could contain spurious line shape components that could be inseparable from the decay of interest, and the photomultiplier could be saturated. Comparatively small transition probabilities in excitation can be overcome by increased laser power, though the use of higher power increases the risk of stimulating other, generally unknown, transitions that could produce cascade effects.

The experimental arrangement is shown in Fig. 1. The

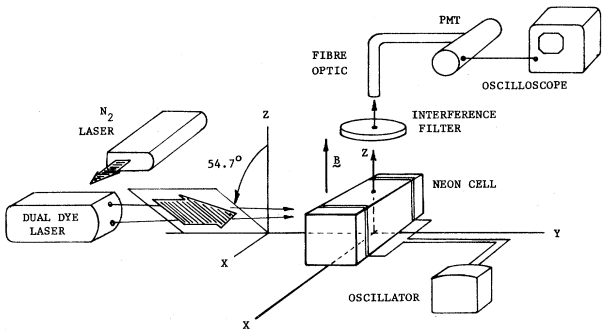

FIG. 1. Experimental layout for two-step lifetime measurements. Certain ancillary equipment such as Helmholtz coils, input polarizer, and reference oscillator are not shown.

laser is a compact nitrogen-pumped dual dye laser based upon a single grating and single dye cell but utilizing beam-splitting optics and separate tuning mirrors.[7] The emergent laser beams consist of 3-ns pulses of 2-GHz spectral width and 10-s^{-1} repetition rate. These beams are attenuated, rotated, repolarized at the magic angle of 54.7° relative to the observation direction, and steered so as to overlap at the neon target. The neon cells consist of five identical $1\times1\times4$ cm^3 quartz cuvettes filled with spectroscopically pure neon. The neon pressures in the cells are determined with a diaphragm-type electronic manometer capable of measuring pressures from 0.1 to 10 Torr with an accuracy of 1.5%. The existence of these cells with fixed and constant pressures greatly facilitated this work because the fluorescence from each of the eight states of interest needed to be measured as a function of neon pressure. These closed cells also eliminated a pressure gradient problem that we encountered in previous work[5] for which the discharge cell remained connected to a large gas-handling manifold. We claim that the sealing of the cells leads to a 5% uncertainty in cell pressure. This claim is based upon extensive measurements of disalignment decay rates $\Gamma^{(2)}$ in the cells and comparison of these results to our previous measurements.[5] Spectral analysis confirms that the sealing of the cells liberated no detectable impurities inside the cell.

The neon cells were located at the center of a pair of Helmholtz coils which produced a magnetic field of about 25 G. Although we observed no effects upon the time-resolved line shapes when we varied, nulled, or reversed the direction of this field, we continued to operate in the field so as to define unambiguously a natural direction of quantization. A 40-MHz oscillator, similar to those that drive optical pumping lamps,[8] was capacitively coupled to the cells in order to drive the electrodeless neon discharge. Under typical operating conditions, the discharge drew about 1 mA of rf current corresponding to a power dissipation of about 150 mW inside the cell. This low-power figure is important in this experiment for two reasons: It is sufficiently small to preclude measurable Stark effects (which we attempted to observe at double or triple these rf levels). The low rf level also permits us to generate sufficient $1s$ populations but at the same time maintain exceptionally low excited-state populations. This latter fact minimizes light trapping in all but the $3s_2$ and $3s_4$ cases, and it also spares the photomultiplier from having to monitor large amounts of dc discharge light.

As discussed in Sec. II, we intentionally refrain from analyzing the polarization of the fluorescence in this experiment, as part of the prescription for suppressing alignment components in the line shape. An appropriate interference filter of $\sim$70 Å FWHM (full width at half maximum) selects from the fluorescent light the particular wavelength of interest. In all cases these spectral lines are well removed from the pumping wavelengths so that we see no laser light mixed into our signals. A 1 m$\times$6 mm diam fiber optic transmits the fluorescent light to a remote Hamamatsu R212UH photomultiplier (PMT) specially selected from the manufacturer's stock to provide good ac linearity of response. The mount for this PMT is wired for fast response and good ac linearity. Linearity tests on this PMT system assure us that signal distortion due to PMT nonlinearity is less than 3%.

As in our previous work,[5] line shape data are captured directly from the screen of a Tektronix 485 350-MHz oscilloscope. The exponentially decaying line shapes are photographed using a single-lens reflex with a 55-mm $f/2$ lens. The oscilloscope's beam intensity and graticule controls are set so that a 15-s time exposure of ASA 400 film through an $f/3.2$ aperture photographically averages about 150 laser shots. Prints measuring 12×17 cm^2 on high-contrast paper provide a permanent record of the line shape. Signal capture by fast transient digitizer would be more convenient but not necessarily more reliable; conversion inaccuracies on all but the most expensive of these instruments are on the order of 5% of full scale, which is comparable to the (CRT) cathode-ray tube inaccuracy in our oscilloscope.

The experimental line shapes are digitized manually using the photographic image of the graticule as a coordinate lattice. The time interval between points on the digitized line shape is 2 or 4 ns; a complete line shape consists of about 45 points. Each set of line-shape photographs includes a shot of 100.000(5)-MHz reference signal displayed on the same portion of the oscilloscope screen that normally contains the fluorescent line shape. By processing these reference shots in the same manner that the fluorescent signals are processed, we calibrate the horizontal graticule to better than 0.5%. Line-shape distortion due to imperfect CRT optics has negligible effect at the current level of accuracy of these measurements. Camera distortion, if present, is immaterial because the digitizing is based upon the image of the graticule contained on the photograph.

IV. DATA REDUCTION AND RESULTS

The raw data were reduced by fitting Eq. (1) to the digitized line shapes. Output from the least-squares-fitting program provided the best overall values for the original amplitude, decay rate $\Gamma^{(0)}$, and base line for each data set. Three separate line shapes at each pressure for each of the eight states were processed. The fits were quite good, the rms residuals being less than 2% of the original amplitude. Figure 2 shows a typical experimental line shape (discrete points) and the least-squares fit (solid line). To test for the presence of spurious components (cascade effects, radio-frequency pickup, PMT ringing, etc.), each set of line-shape data was reduced one point at a time (starting at $t=0$) and then refit until only 50% of the original data set remained. In most instances the succession of fitted parameters showed no strong trends, thereby substantiating our claim that all important spurious effects have been adequately suppressed. Fluorescent line shapes from several states (the $4d'_1$, $4d''_1$, and $4s''_1$) not reported here did not pass this test; hence we are still working on them.

The values of $\Gamma^{(0)}$ returned by the least-squares fits are plotted in Fig. 3 as a function of neon pressure P, with the pressure ranging from 0.85(0.04) to 7.7(0.4) Torr. The straight lines passing through these data permit us to determine the decay gradients β and the unperturbed lifetimes τ from the zero-pressure intercepts γ_b. The results

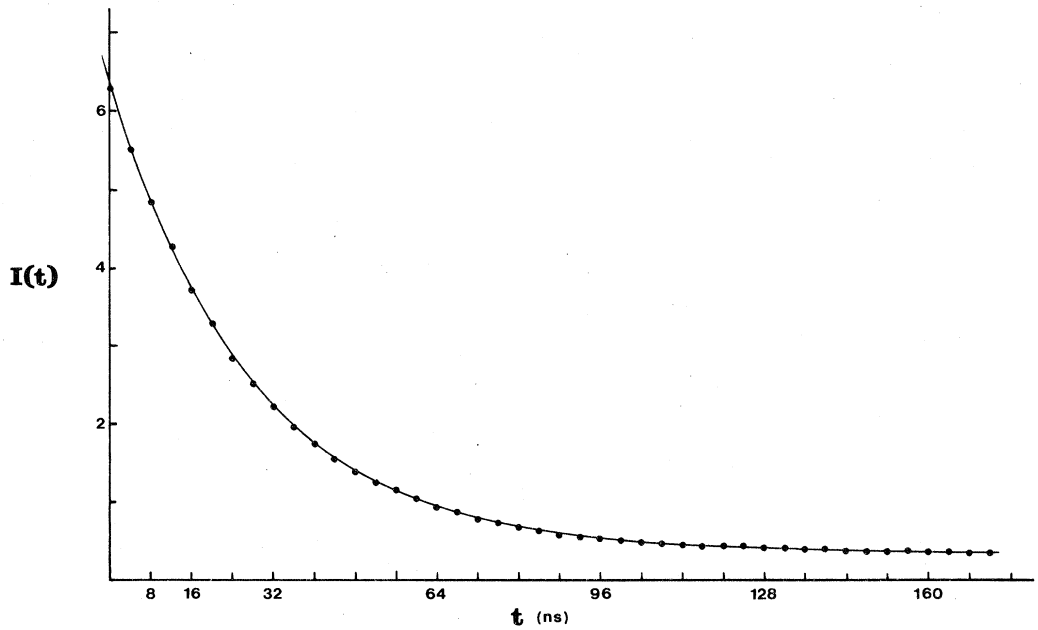

FIG. 2. Typical time-resolved experimental line shape showing the exponential decay of the fluorescent light intensity $I(t)$ in arbitrary units vs time t in ns after the laser pulses. Dots represent the digitized experimental line shape; the solid line is the least-squares-fitted line shape. This particular trace represents the 5341.1-Å emission from the $4d_5$ state at a pressure of 0.85 Torr. The fitted decay constant is $\Gamma^{(0)}=36.0(0.6)$ Mrad/s and the baseline is 0.35 arbitrary units.

are collected in Table II and compared to the work of others, both experimental and theoretical. The quoted uncertainties in our lifetimes and cross sections represent a combination of statistical and systematic uncertainties. The largest single contributor to the overall uncertainty is the 5% uncertainty in the neon pressures.

V. DISCUSSION

The adequacy of the least-squares fits, as shown in Fig. 2, and the straightness of the $\Gamma^{(0)}$ vs P contours in Fig. 3 lends support to the analysis of Sec. II: polarization and cascade effects, which manifest themselves in beats and/or impure decays, can indeed be suppressed even in a discharge environment. To consider the matter of light trapping, we take up the $3s_2$ and $3s_4$ states first. These states are unique among our eight because they show strong transition probabilities ($\sim 0.5\times 10^8$ s^{-1}) for decay directly to the $1P_0$ ground state, which contains virtually 100% of the neon atoms in our samples. It follows that for our range of pressure, light trapping on these $3s_{2,4}\leftrightarrow 1P_0$ resonance lines is complete or "saturated." Decomps and Dumont have studied this effect carefully.[9] They find that complete light trapping leads to a uniform depression (downward translation) of the $3s_2\Gamma^{(0)}$ vs P contour by 37(3) Mrad/s. If we assume their value of 19.6(0.6) ns for the lifetime of the $3s_2$ state, we find that our $\Gamma^{(0)}$ vs P contour is depressed by a similar amount of 40(3) Mrad/s. No doubt a similar shift exists for the $3s_4$ contour. Since we cannot operate our discharge at sufficiently low pressures to escape from the light-trapping regime, we cannot infer γ_b or τ for the $3s_2$ or $3s_4$ states. It is for this reason that the $3s_2$ and $3s_4$ lines in Fig. 3 have not been extended to the vertical axis; data at lower pressures would show, in fact, that these contours turn up sharply at $P=0.3$ Torr.[9] But since the effect of saturated light trapping does not alter the slope of the $\Gamma^{(0)}$ vs P contour, we can infer collision cross sections for these states as shown in Table II. The agreement with previous values of $\sigma^{(0)}$ for the $3s_2$ state is satisfactory; unfortunately, theoretical values are nonexistent.

The remaining six states suffer negligible light-trapping effects because they are not connected directly to the ground or $1s_{2,3,4,5}$ pseudo-ground-states, which are the only states with sizable populations in our weak discharge. In previous work using the same cells and discharge conditions,[5] we were able to measure only small amounts of light trapping in the relaxation of the $2p_2$ and $2p_5$ states to the $1s_3$ state, even though the transition probabilities are large and the $1s_3$ state is metastable (hence highly populated in a relative sense). We are certain, therefore, that under the same conditions (which exist in the current experiment), we would not be able to detect light trapping for the six states of interest because their $\gamma_{bc}x_{bc}$ products in Eq. (2) are at least an order of magnitude smaller.

One can see in the second column of Table II that the lifetimes in the current work are in good agreement with the recent measurements of Martin and Campos but in serious disagreement with the older values of Osherovich and Verolainen. In the latter case we can think of no reason why our smaller lifetimes should be faulty. Failure on our part to account for unanticipated light trapping

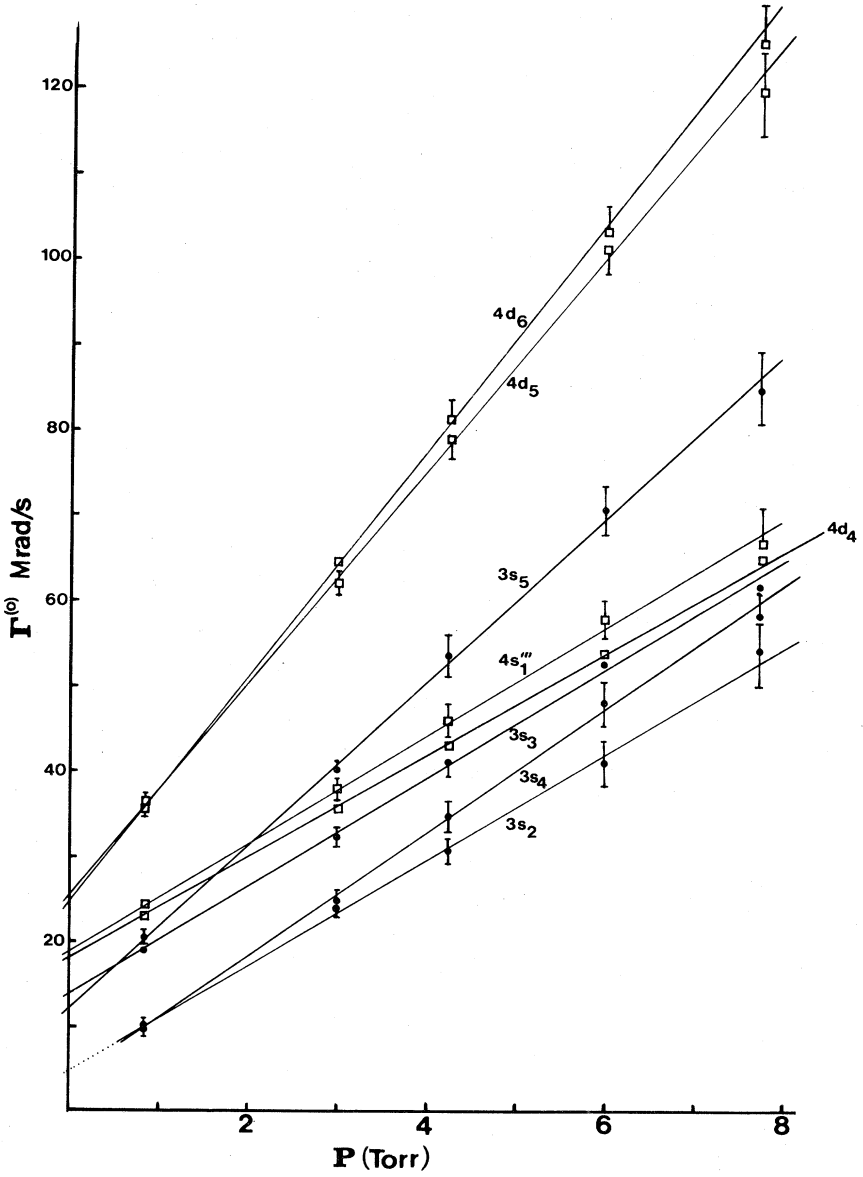

FIG. 3. Plots of population decay rate $\Gamma^{(0)}$ in Mrad/s vs neon pressure P in Torr for eight states of interest. All data points for the $3s_2$ and $3s_4$ states have been displaced downwards by 7.50 Mrad/s to minimize overlap and confusion. Missing error bars are similar to those shown at the same pressure.

would only accentuate the discrepancy. As shown in Fig. 2, the fits to the $4d_5$ line shapes were exceptionally good; there is no hint of a longer-lived component that might be the true decay of the $4d_5$ state. For these reasons we conclude that the 104-ns lifetime values of Osherovich and Verolainen are suspect.

Our experimental lifetimes are also in good agreement with the theoretical values collected in the fourth column of Table II, except possibly in the case of the $4d_6$ state where the agreement is less satisfactory. The theoretical lifetimes superscripted by the letter "b" were calculated by Gruzdev and Loginov, who took configuration overlap into account. The values quoted in Table II supersede values published a few years earlier by the same authors.[10] In the case of the $4d_6$ state, the earlier lifetime values were 44.7, 44.8, and 46.5 ns depending upon the type of transition integrals and the number of configurations taken into account. The present work suggests that the earlier calculations may in fact have been the more reliable.

Since seven of the eight collision cross sections have not been measured previously, and theoretical values for these cross sections have not been attempted, we have no comparisons at present for the values of $\sigma^{(0)}$ quoted in the last column of Table II. It is interesting to note, however, that the cross section for the $3s_5$ state is significantly greater than that of its neighboring $3s$ states, and the absolute

TABLE II. Results of current investigation and comparison with experimental and theoretical work of others.

State of interest	Lifetime (expt.) (ns) This work	Lifetime (expt.) (ns) Others	Lifetime (theory) (ns) Others	Decay gradient β (Mrad s^{-1} $Torr^{-1}$) This work	Cross section $\sigma^{(0)}$ ($Å^2$) This work	Cross section $\sigma^{(0)}$ ($Å^2$) Others
$3s_5$	81(6)	80(8)[a]	78.4[a]; 77.1(7.0)[b]	9.6(0.8)	40(3)	
$3s_4$		19.5(0.5)[c]	19.6(2.0)[b]	7.2(0.9)	30(4)	
$3s_3$	73(5)		78.7(8.0)[b]	6.3(0.6)	26(3)	
$3s_2$		23.1(1.5)[c]	25.4(3.0)[b]	6.2(0.6)	26(3)	20(10)[d]
		19.6(0.6)[e]				23(5)[e]
$4d_6$	41(4)	104(3)[f]	52.2(5.0)[b]	13.3(1.0)	56(4)	
$4d_5$	39(4)	104(3)[f]	34.0(3.0)[b]	12.5(1.0)	52(4)	
$4d_4$	55(5)	59(6)[a]	57.6[a]; 57.4(6.0)[b]	6.0(1.0)	25(4)	
$4s_1'''$	53(6)		57.3(6.0)[b]	6.3(1.0)	26(4)	

[a]P. Martin and J. Campos, J. Phys. B 10, 1265 (1977).
[b]P. F. Gruzdev and A. V. Loginov, Opt. Spectrosc. (USSR) 45, 846 (1978).
[c]G. M. Lawrence and H. S. Liszt, Phys. Rev. 178, 122 (1969).
[d]S. A. Kazantsev and V. I. Eiduk, Opt. Spectrosc. (USSR) 45, 735 (1978).
[e]B. Decomps and M. Dumont, IEEE J. Quantum Electron. 4, 916 (1968).
[f]A. L. Osherovich and Y. F. Verolainen, Opt. Spectrosc. (USSR) 22, 181 (1967).

sizes of the $4d_5$ and $4d_6$ cross sections are nearly double those of the neighboring states.

In conclusion, we have measured lifetimes and collisional quenching cross sections for eight states in the $2p^5 5s$ and $2p^5 4d$ manifolds of neon by exploiting stepwise excitation of atoms in a weak discharge. We have shown that the usual problems associated with lifetime measurements can be avoided. The experimental values of the lifetimes are in good agreement with the recent work of others, both experimental and theoretical. The experimental cross sections stand ready for comparison to theory.

ACKNOWLEDGMENTS

We are pleased to acknowledge support from Research Corporation, the National Science Foundation, and Lawrence University. The lasers used in this work were constructed by H. W. Everson. Preliminary versions of this experiment were developed by D. C. DeMets and E. J. Dehm; the author is pleased to acknowledge their contributions.

[1]J. N. Dodd and G. W. Series, *Progress in Atomic Spectroscopy,* edited by W. Hanle and H. Kleinpoppen (Plenum, New York, 1978), Part A, p. 639.
[2]S. Haroche, *Quantum Beats and Time-resolved Spectroscopy,* Vol. 13 of *Topics in Applied Physics,* edited by K. Shimoda (Springer, Berlin, 1976), p. 253.
[3]I. Tanarro, F. Arqueros, and J. Campos, Phys. Rev. A 27, 2533 (1983).
[4]E. J. Dehm and J. R. Brandenberger, Bull. Am. Phys. Soc. 28, 788 (1983).
[5]J. R. Brandenberger and B. R. Rose, Opt. Commun. 36, 453 (1981).
[6]W. L. Wiese and G. A. Martin, *Wavelengths and Transition Probabilities for Atoms and Atomic Ions, Part II,* Natl. Stand. Ref. Data Ser., Natl. Bur. Stand. (U.S.) Circ. No. 68 (U.S. GPO, Washington, D.C., 1980).
[7]J. R. Brandenberger (unpublished).
[8]W. E. Bell, A. L. Bloom, and J. Lynch, Rev. Sci. Instrum. 32, 688 (1961).
[9]B. Decomps and M. Dumont, IEEE J. Quantum Electron. 4, 916 (1968).
[10]P. F. Gruzdev and A. V. Loginov, Opt. Spectrosc. (USSR) 35, 1 (1973).